Improving Oxygen Barrier Properties of Poly(ethylene Terephthalate) by Incorporating Isophthalate. I. Effect of Orientation

R. Y. F. Liu,[1*], Y. S. Hu,[1] M. R. Hibbs,[2] D. M. Collard,[2] D. A. Schiraldi,[1] A. Hiltner,[1] and E. Baer[1]

[1]*Department of Macromolecular Science and Center for Applied Polymer Research, Case Western Reserve University, 10900 Euclid Avenue, Cleveland, Ohio 44106-7202*
[2]*School of Chemistry and Biochemistry, Georgia Institute of Technology, Atlanta, Georgia 30332*

Received 4 January 2005; accepted 28 February 2005
DOI 10.1002/app.22213
Published online in Wiley InterScience (www.interscience.wiley.com).

ABSTRACT: The present study examined poly(ethylene terephthalate) (PET) and a series of statistical and blocky copolymers in which up to 30% of the terephthalate was replaced with isophthalate by copolymerization and melt blending, respectively. Some level of transesterification during processing of melt blends resulted in blocky copolymers, as confirmed by NMR. Random and blocky copolymers exhibited similar properties in the glassy state, including a single glass transition, due to miscibility of the blocks. However, random copolymerization effectively retarded cold-crystallization from the glass whereas blocky copolymers readily cold-crystallized to a crystallinity level close to that of PET. The polymers were oriented at four temperatures in the vicinity of the T_g and characterized by oxygen transport, wide-angle X-ray diffraction, positron annihilation lifetime spectroscopy, and infrared spectroscopy. Orientation of all the copolymers resulted in property changes consistent with strain-induced crystallization. However, blocky copolymers oriented more easily than random copolymers of the same composition and after orientation exhibited slightly lower oxygen permeability, higher density, and higher fraction *trans* conformers. Analysis of oxygen solubility based on free volume concepts led to a two-phase model from which the amount of crystallinity and the amorphous phase density were extracted. Dedensification of the amorphous phase correlated with the draw temperature. J Appl Polym Sci 98: 1615–1628, 2005

Key words: poly(ethylene terephthalate); polyester blends; copolyesters; orientation; oxygen permeation; diffusion

INTRODUCTION

Poly(ethylene terephthalate) (PET) is widely used in a range of high-barrier applications because of its low cost and good mechanical properties. Additional applications only await further improvement of the gas barrier properties. Isomeric poly(ethylene isophthalate) (PEI) has significantly lower oxygen permeability than PET, close to that of PEN.[1] Copolymerization with isophthalate offers one approach to increasing the gas barrier of PET. A small amount of isophthalate is often incorporated into PET to retard thermal crystallization.[2,3] The larger amount of isophthalate that would be required to significantly impact gas permeability would also reduce T_g[1] and could affect processing performance. High orientation and strain-induced crystallization induced by the stretch-blow molding process impart good gas barrier to PET bottles.[4] The possibility exists that significant levels of isophthalate would adversely affect orientation and crystallization.

Solid-state structure and properties can be manipulated by altering chain distribution of the higher barrier comonomer. Polyester blends undergo transesterification over time in the melt, eventually forming the statistical copolymer.[5] However, the process is slow enough that blocky copolymers can be obtained by melt blending the corresponding homopolymers for a certain period of time. This was demonstrated with blends of PET and a frustrated liquid crystalline polyester of bibenzoic acid.[6] In comparison with randomly distributed bibenzoate groups, the same amount of bibenzoate as frustrated liquid crystalline blocks formed small domains in the quenched glass. Subsequent drawing of the blocky structure demonstrated advantages including enhanced chain orientation, a larger processing window, and orientation at higher draw temperatures without significant chain relaxation.

Considering that the PET bottle wall experiences both crystallization and orientation during the blowing process, it is not surprising that the relationship between gas transport and solid-state structure is a complex one. In addition to being an important performance property, oxygen permeability becomes a

Correspondence to: A. Hiltner (pah6@po.cwru.edu).
*Present address: 3M, St. Paul, MN 55144.
Contract grant sponsor: KoSa.

powerful structural probe when separated into its thermodynamic and kinetic components of gas solubility and gas diffusivity.[7] Analysis of oxygen solubility by free volume concepts provides a reliable measure of bottle wall crystallinity and reveals fundamental characteristics of the amorphous phase, such as amorphous phase density and amorphous phase oxygen solubility.[8] The structural insight can be the basis for process optimization.

In the present study, up to 30% isophthalate was incorporated into PET as either a random copolymer or a blocky copolymer. Statistical copolymers were achieved by copolymerization. A blocky distribution was achieved by melt blending the homopolymers, PET and PEI. The effect of comonomer distribution on thermal behavior, orientation, and oxygen barrier properties was examined. The results were analyzed in terms of free volume concepts developed previously.[8]

METHODS

Materials

Pellets of PET, PEI, and statistical copolymers with 10, 20, and 30% isophthalate (PET-*co*-10I, PET-*co*-20I, and PET-*co*-30I, respectively) were supplied by KoSa (Spartanburg, SC). The copolymers were polymerized according to the methodology described previously.[1] The intrinsic viscosity measured at 25°C in 1% (w/w) dichloroacetic acid solution was 0.60, 0.58, and 0.53 dL g^{-1} for PET-*co*-10I, PET-*co*-20I, and PET-*co*-30I, respectively, based on the coefficient for PET. Blends of PET and PEI with composition PET/PEI 90/10, 80/20, and 70/30 (w/w) (PET-*b*-10I, PET-*b*-20I, and PET-*b*-30I, respectively) were prepared by coextrusion in a Rheocord 90 twin-screw extruder at 285°C. The PET and PEI used for blending had intrinsic viscosities of 0.84 and 0.75 dL g^{-1}, respectively.

Pellets were dried *in vacuo* at 80°C for 24 h, compression-molded, and quenched into amorphous films as described previously.[9,10] The temperature of the press was 265°C. Films 180 and 600 μm in thickness were prepared.

The 600-μm-thick amorphous films were stretched under constrained uniaxial conditions. The specimen width before stretching was 130 mm and the gauge length was 32 mm. A grid was marked on the specimen for measuring the draw ratio before the specimen was clamped between wide grips and mounted in the environmental chamber of an Instron machine. Specimens were stretched at four draw temperatures T_d with respect to the glass transition temperature T_g. The draw rate was 50 mm min^{-1} at T_g + 30°C and T_g + 15°C. The draw rate was 5 mm min^{-1} at T_g and T_g − 15°C, except for PET-*co*-20I and PET-*co*-30I. Lower draw rates were required at T_g and T_g − 15°C to prevent fracture of these compositions. All specimens were stretched to a strain of 300% to achieve a target draw ratio of 4. The actual draw ratio was determined from the grid marked on the specimen. All films remained transparent after drawing. The final thickness was 100–200 μm. The 180-μm-thick quenched films served as controls.

Characterization

Blends of PET and PEI were analyzed by ^{1}H-NMR spectroscopy to determine their compositions and by ^{13}C-NMR spectroscopy to determine the randomness of the sequence of terephthalate (T) and isophthalate (I) structural units. Sample concentrations were 20 mg mL^{-1} in a mixture of hexafluoroisopropanol and $CDCl_3$ (approximately 5/95 v/v). Chemical shifts were measured with respect to internal tetramethylsilane. The ^{1}H- and ^{13}C-NMR spectra were acquired on a Bruker AMX 400-MHz instrument operating at 400.1 and 100.6 MHz, respectively. The spectral width was 18 kHz, the relaxation delay was 2 s, and inverse gated decoupling was used to eliminate the nuclear Overhauser effect. A deconvolution program in the NMR software was used to integrate ^{13}C-NMR spectra.

Differential scanning calorimetry (DSC) was performed on 180-μm-thick quenched films with a Perkin-Elmer DSC-7 calibrated with indium and tin standards. All tests were performed in a nitrogen atmosphere with heating rate of 10°C min^{-1}. The heat capacity jump ΔC_p at T_g was determined as described previously.[11]

Two-dimensional wide-angle X-ray scattering (WAXS) of drawn films was carried out using a Philips PW1830 X-ray source fitted with a digital image plate. The X-ray pattern was recorded with a resolution of 3700 × 3000 pixels.

Dynamic mechanical thermal analysis (DMTA) on quenched 180-μm-thick films was carried out in a DMTA Mk II unit from Polymer Laboratories (Amherst, MA) operating in the tensile mode. Measurements were taken over a temperature range of −150 to 125°C. The heating rate was 3°C min^{-1} and the frequency was 1 Hz.

A density gradient column was constructed from a solution of calcium nitrate and water in accordance with ASTM D Standard 1505 Method B. The column was calibrated with glass floats of known density. Small pieces of quenched and oriented films (ca. 25 mm^2) were placed in the column and allowed to equilibrate for 30 min at 23°C before measurements were taken. Averages of four measurements are reported. The accuracy was ±0.0009 g cm^{-3}.

Conformational composition was determined with photoacoustic Fourier transform infrared spectroscopy as described previously.[12] Spectra were collected at ambient temperature with a Nicolet 870 Fourier transform infrared spectrometer with an MTEC Model

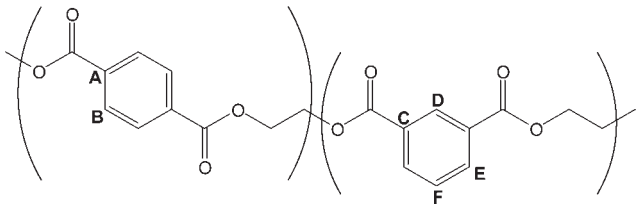

Scheme 1

No. 200 photoacoustic cell. Specimens were dried *in vacuo* at ambient temperature to remove moisture. For each specimen, 256 scans were collected at a resolution of 4 cm^{-1} and a mirror velocity of 0.158 cm s^{-1}. The 1500–1400 cm^{-1} region of the spectrum was deconvoluted into three Gaussian peaks with Origin 4.1 software. The fractions of *gauche* and *trans* glycol conformers were obtained from the appropriate peak heights.

Positron annihilation lifetime spectroscopy (PALS) employed a fast-fast coincident method with a time resolution of 230 ps, which has been described in detail elsewhere,[13] at a count rate of approximately 10^6 counts h^{-1}. The positron lifetime τ was determined by PATFIT software. The positron annihilation spectra were fitted to three exponentially decaying lifetime components. The longest lived component, with lifetime τ_3, corresponded to the pickoff annihilation of *o*-Ps in the free-volume holes of the polymer matrix, from which the mean hole radius *r* was calculated.[13] The uncertainty in *r* based on 10 spectra was ± 0.02 Å.

Oxygen flux $J(t)$ at 0% relative humidity, 1 atm pressure, and 23°C was measured with a MOCON OX-TRAN 2/20. Specimens were carefully conditioned as described previously.[9] Diffusivity *D* and permeability *P* were obtained by fitting the nonsteady state flux–time curve to the solution to Fick's second law with appropriate boundary conditions.[9] The thickness *l* of each specimen was determined from the measured density after the barrier measurement was completed. Most of the specimens were tested within 1–3 days after orientation. However, testing after 30 days produced the same flux, suggesting that the specimens were fully relaxed soon after orientation.[12]

RESULTS

Copolymer composition and sequence distribution

The composition of PET/PEI blends was determined by comparing the integrals of the signals in the ^{1}H-NMR spectra arising from the terephthalate protons (B) to those arising from the protons meta to the ester groups of the isophthalate units (F). This analysis confirmed that the ratio of terephthalate units to isophthalate units was within 2% of the molar ratio of the two homopolymers used in the blending procedure (Scheme 1).

A similar study of a random copolymer, poly(ethylene terephthalate-*co*-isophthalate), showed that the quaternary carbons (A and C) are sensitive to the identity of the adjacent structural units and can thus be used to measure the relative amounts of triad and dyad sequences.[14] Another study of terpolyesters containing 5-*tert*-butylisophthalic units showed that the carbon atom that is meta to the two ester groups in the 5-*tert*-butylisophthalic units is also sensitive to backbone sequence.[15] These previous studies simply confirmed that copolymerization leads to random copolymers. In the case of our PET/PEI blends we used the sensitivity of ^{13}C-NMR chemical shifts to adjacent units to determine the randomness of the sample and to follow the evolution of structure as two homopolymers undergo transesterification to form a random copolymer.

The ipso carbons of the terephthalate structural units (A) give rise to four peaks in the ^{13}C-NMR spectra of the PET/PEI blends. The two peaks with chemical shifts of δ 133.72 and 133.69 ppm are due to the ITI and TTT triad sequences, respectively (Figure 1). The remaining two peaks, with chemical shifts of δ 133.76 and 133.66 ppm, are due to carbon A of the asymmetrically substituted terephthalate units in the TTI triad sequence. The quaternary carbons in the isophthalate units (C) also give rise to four peaks due to triad sequences, but they are not resolved well enough to integrate separately. The carbons meta to the ester groups of the isophthalate structural units (F) give rise to three peaks in the spectrum. The peaks at δ 129.13, 129.11, and 129.08 ppm are due to the TII, TIT, and III triad sequences, respectively. These assignments were made by comparing the integral ratios from samples of the random copolymers. The relative amounts of the triad sequences could be predicted for any given composition of random copolymer and these triads could then be assigned to the peaks in the ^{13}C-NMR spectra by noting how the peak integrals changed as the composition of the copolymer changed.

The relative integrations of these peaks can be used to determine the amount of transesterification that occurs during extrusion. If the two polymers do not react at all, the ^{13}C-NMR spectrum will only have peaks for the TTT and III triads. As transesterification occurs, a block copolymer is formed and the peaks for the other four triads will appear in the spectrum. If the two polymers completely randomize during extrusion, these peaks will have integral ratios matching those calculated on the basis of a Bernoullian statistical model for a random copolymer with the same composition.

The differences in chemical shift between some of these peaks are small and consequently some of the peaks overlap one another and cannot be integrated separately. If at least one of the peaks arising from a

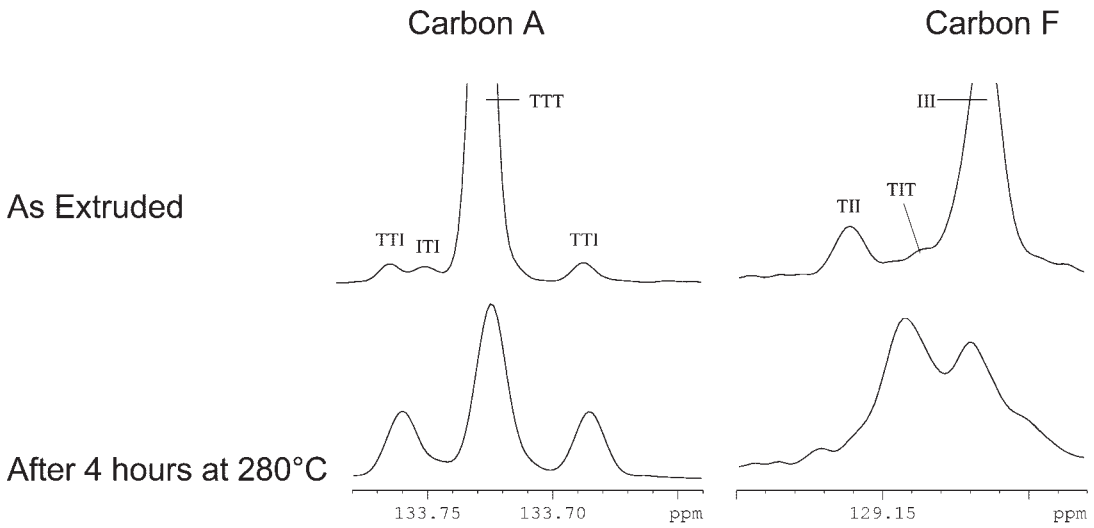

Figure 1 Aromatic region of ^{13}C-NMR spectra of the PET-*b*-30I blend showing multiple signals for carbon A (terephthalate ipso) and carbon F (isophthalate C-5) due to triad sequences.

particular type of carbon is well resolved, dyad information can be determined by expressing the area of one peak as a fraction of the total area of all the peaks due to that particular carbon. For example, if the relative amounts of terephthalate-based dyads (TI and TT) are designated: $P_{TI} = X$ and $P_{TT} = 1 - X$. Then the ratios of the terephthalate-centered triads (TTT, ITI, and TTI) are

$$P_{TTT} = (1 - X)^2 \quad (1)$$

$$P_{ITI} = X^2 \quad (2)$$

$$P_{TTI} = 2X(1 - X)\,. \quad (3)$$

Any one of these equations (or combinations of them) can be used to solve for X by setting it equal to the relative area of its corresponding peak (or the sum of the areas of the corresponding peaks). A similar analysis of the isophthalate-centered triads gives the values for P_{IT} and P_{II}. The degree of randomness, R, is then calculated:[16]

$$R = P_{TI} + P_{IT}\,. \quad (4)$$

The quantity R is used to describe the randomness of copolymers formed upon blending: For a physical blend of PET and PEI homopolymers without transesterification, $R = 0$. For a random copolymer, $R = 1$ (using this analysis, $R = 2$ for an alternating copolymer).

Table I shows the measured values of R for the coextruded blends of PET and PEI. The low values (0.1, 0.1, and 0.2 for the 70/30, 80/20, and 90/10 blends, respectively) for the as-extruded samples indicated that relatively little transesterification occurred during blending. Accordingly, the blended materials more closely resembled block copolymers than random copolymers or physical blends. Processing of the blends into films and orientation of those films had little, if any, further effect on the blockiness. The blends randomized with further heat treatment as shown by a sample of the 70/30 blend, which had an R value of 0.93 after it was held for 4 h at 280°C (Figure 1). A sample of the random copolymer PET-*co*-10I (prepared copolymerizing terephthalate and isophthalate monomers) was also examined and the degree of randomness was determined to be near the expected value of 1.0 for both

TABLE I
Experimental and Theoretical Sequence Distribution (*R*)

Thermal history	PET-*co*-10I	PET-*b*-10I	PET-*b*-20I	PET-*b*-30I
As prepared	1.2	—	—	—
As extruded	—	0.2	0.1	0.1
Quenched film	1.1	0.3	0.2	0.1
Oriented film (at T_g)	—	0.2	0.2	0.1
After 4 h at 280°C	—	—	—	0.9

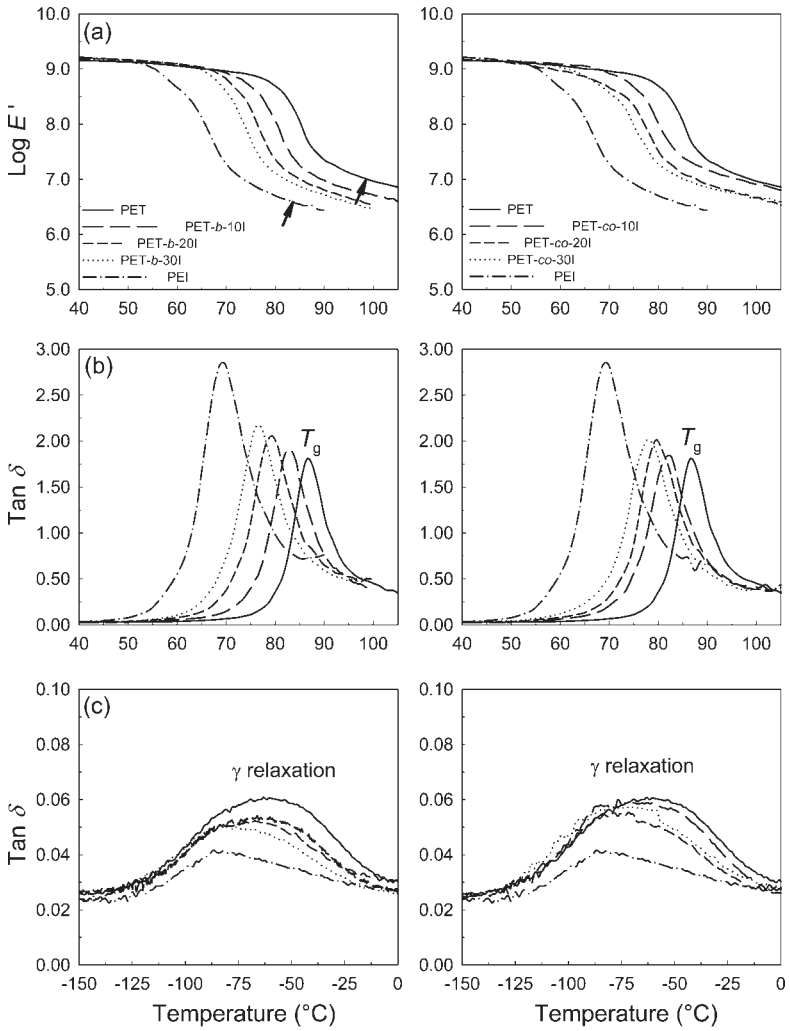

Figure 2 Dynamic mechanical behavior of quenched polyester films: (a) Log E'; (b) tanδ (T_g); (c) tanδ (γ-relaxation).

the copolymer resin and a quenched film prepared from the resin (Table I).

Thermal properties and free volume

The dynamic mechanical properties of homopolymers and copolymers are compared in Figure 2. The strong relaxation peak in the tanδ curve and large accompanying drop in logE' were identified with the glass transition. The relaxation intensity as characterized by the maximum in tanδ increased from 1.8 for PET to 2.8 for PEI. The correspondingly larger modulus drop for PEI was due to a lower plateau modulus E_0. This corresponded to lower entanglement density M_e according to[17]

$$M_e = \frac{3\rho RT}{E_o}, \qquad (5)$$

where ρ is the density in the rubbery state; R is the gas constant; and T is the absolute temperature. To calculate M_e for PET and PEI, E_0 was taken at the temperature corresponding to the end of the tanδ peak, as indicated by the arrows in Figure 2(a). The calculated M_e according to eq. (5) was higher for PEI (Table II), which was attributed to its smaller coil size as revealed by molecular dynamics simulations.[18] The higher fraction of *trans* conformers in PEI (0.25) compared to PET (0.08) was responsible for the smaller coil size of PEI and thus its denser packing. It appeared that chain kinks imparted by isophthalate facilitated the *trans* glycol conformation.

The quenched PET film exhibited a broad subambient γ-relaxation centered at about −75°C. The γ-relaxation of PEI was much weaker and shifted to lower temperature. It was previously suggested that asymmetric substitution of the phenyl ring limited local segmental motions responsible for the γ-relaxation.[19] Molecular simulations confirmed significantly lower segmental mobility of phenyl rings in PEI compared to PET and moreover demonstrated that lower oxygen diffusivity of PEI was a direct

TABLE II
Physical Properties of PET and PEI

Polymer	Density (g cm^{-3})	$\Delta\alpha$ (α_1-α_g) (cm^3 g^{-1}K^{-1})	ΔC_p ($C_{pl}-C_{pg}$) (J g^{-1} K^{-1})	T_g (DSC) (°C)	P	D	S	r (Å)	Log E_0 (E_0 in Pa)	M_e (kg mol^{-1})
PET	1.3370	3.6–5.2[a]	0.38	76	0.424	5.0	0.098	2.56	7.0	1.1
PEI	1.3464	1.8–3.3[a]	0.42	55	0.090	1.7	0.061	2.41	6.7	2.5

Note. P, cc cm m^{-2} day^{-1} atm^{-1}; D, 10^{-13} m^2 s^{-1}; S, cc cm^{-3} atm^{-1}.
[a] Ref. [23].

consequence of reduced segmental mobility.[18,20] The relationship between γ-relaxation intensity and oxygen diffusivity has been verified experimentally for aromatic polyesters.[1,21]

Despite the blocky chain structure of blocky copolymers, as indicated by NMR, only a single glass transition peak was observed. Peak temperature T_g and peak intensity were identical for random and blocky copolymers of the same composition (Table III), which indicated that the PET and PEI blocks were completely miscible. Within the resolution of the spectra, the γ-relaxation intensity and peak temperature decreased with isophthalate concentration in the same way for random and blocky copolymers.

Thermograms of the copolymers exhibited a single glass transition inflection (Figure 3). The inflection temperature showed the same dependence on copolymer composition regardless of whether the distribution was blocky and random (Table III). Subsequent discussion of T_g is based on DSC values. The composition dependence of the glass transition of miscible polymer blends is often described by the Gordon–Taylor equation as[22]

$$T_g = \frac{\omega_l T_{g1} + K\omega_2 T_{g2}}{\omega_1 + K\omega_2}, \qquad (6)$$

where T_g is the copolymer glass transition temperature; ω_1 and ω_2 are the weight fractions of ethylene terephthalate and ethylene isophthalate, respectively; and T_{g1} and T_{g2} are the glass transition temperatures of PET and PEI, respectively. Results for copolymers fit eq. (6) with $K = 2.0$ (Figure 4). The constant K is identified either as the ratio of thermal expansivity differences $\Delta\alpha_2/\Delta\alpha_1$ of the homopolymers,[22] where $\Delta\alpha = \alpha_l$-α_g, is the difference between the thermal expansivities of the liquid and glass, or as the ratio of heat capacity differences at T_g, $\Delta C_{p1}/\Delta C_{p2}$,[23] where $\Delta CP = C_{pl} - C_{pg}$, is the difference between the heat capacities of the liquid and glass. The values of $\Delta\alpha$[24] and ΔCp for PEI and PET (Table II) give ratios of about 0.6 for thermal expansivity and 1.1 for heat capacity. Neither approach predicts the experimental value of K for the copolymers in this study.

According to free volume concepts, decreasing T_g should result in lower free volume of the glass at ambient temperature. This is apparent in the gradually decreasing free volume hole size from PALS (Table III). The effect can be expressed in terms of specific volume according to

$$\Delta\nu = \Delta T_g \Delta\alpha, \qquad (7)$$

where $\Delta\nu$ is the difference in specific volume relative to PET, ΔT_g is the difference in glass transition temperature relative to PET, and $\Delta\alpha$ is the thermal expansivity difference between the rubbery and glassy states. Taking an average value of $\Delta\alpha = 3.0 \times 10^{-4}$ cm^3 g^{-1} K^{-1},[24] good correlation was found between $\Delta\nu$ from eq. (7) and the measured value from the density in Table III.

TABLE III
Thermal Properties of Quenched Films

		DMTA	DSC								
Polymer	ρ (g cm^{-3})	T_g (°C)	T_g (°C)	T_{cc} (°C)	ΔH_{cc} (J g^{-1})	T_m (°C)	ΔH_m (J g^{-1})	$\Delta\nu$ (cm^3 g^{-1})	$\Delta T_g\Delta\alpha$ (cm^3 g^{-1})	r (Å)	f_t
PET	1.3370	86	76	140	34	246	35	0.000	0.000	2.56	0.08
PET-*co*-10I	1.3396	84	72	151	31	233	32	0.145	0.120	2.52	0.09
PET-*co*-20I	1.3406	79	68	171	1.4	205	1.2	0.201	0.240	2.49	0.10
PET-*co*-30I	1.3410	77	66	—	—	—	—	0.223	0.300	2.48	0.11
PET-*b*-10I	1.3388	83	72	134	33	245	34	0.101	0.120	2.51	0.08
PET-*b*-20I	1.3406	80	69	134	32	243	34	0.201	0.210	2.48	0.09
PET-*b*-30I	1.3429	78	65	139	28	240	29	0.329	0.330	2.46	0.11
PEI	1.3464	69	55	—	—	—	—	0.522	0.630	2.41	0.25

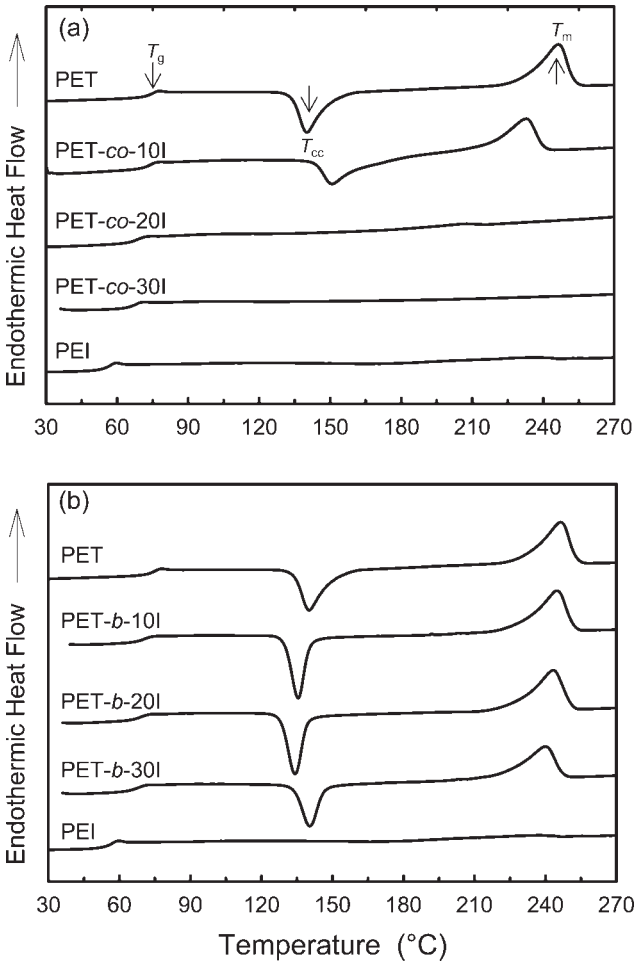

Figure 3 First heating of quenched polyester films: (a) random copolymers; (b) blocky copolymers. The heating rate was 10°C min^{-1}.

Although random and blocky copolymers both formed homogeneous glasses, they differed considerably in their cold-crystallization behavior (Figure 3). Random inclusion of isophthalate groups significantly retarded crystallization of PET from the glassy state as indicated by the increase in cold-crystallization temperature T_{cc} from 140 to 151°C for PET-*co*-10I and a decrease in crystallization enthalpy ΔH_{cc} from 34 to 31 J g^{-1}. The decrease in melting temperature from 246 to 233°C indicated that the crystals were smaller and more defective than in homopolymer PET. Cold-crystallization of PET-*co*-20I was barely discernable at a heating rate of 10°C min^{-1}. The T_{cc} increased to 171°C and the crystallization enthalpy concurrently decreased to 1.4 J g^{-1} (Table III). The small crystal fraction melted at 205°C. Neither crystallization nor melting was detected in heating thermogram of PET-*co*-30I. Similar trends were observed previously with other random copolymers of PET.[25] Correspondence in the enthalpies of crystallization and melting confirmed the amorphous nature of the quenched films (Table III).

In contrast to random copolymers, blocky copolymers readily cold-crystallized. The blocky copolymers actually crystallized faster than PET, as indicated by slightly lower T_{cc} (Table III). The enthalpies of cold-crystallization and melting did not reduce in proportion to terephthalate content. Compared to 34 J g^{-1} for ΔH_{cc} of PET, PET-*b*-10I, PET-*b*-20I, and PET-*b*-30I had ΔH_{cc} of 33, 32, and 28 J g^{-1}, respectively. Likewise, ΔH_m of PET-*b*-10I, PET-*b*-20I, and PET-*b*-30I was 34, 34, and 29 J g^{-1}, respectively, whereas ΔH_m of PET was 35 J g^{-1}. It is speculated that PEI blocks cocrystallized with PET to some extent.

Orientation by cold- and hot-drawing

Quenched films were drawn to a target strain of 300% to achieve a target draw ratio of 4 at four temperatures with respect to the T_g: at $T_g - 15$°C, at T_g, at $T_g + 15$°C, and at $T_g + 30$°C. The PET film drawn at $T_g - 15$°C showed a WAXD pattern typical of an oriented glass with equatorial concentration of the amorphous halo intensity [Fig. 5(a)]. The absence of crystalline reflections in this pattern was in agreement with previous observations[26] and confirmed the noncrystalline nature of the oriented PET.[27] The process of molecular orientation at $T_g - 15$°C without strain-induced crystallization is referred to as cold-drawing.

Films drawn at or above T_g exhibited some level of crystallinity as indicated by crystalline reflections in the WAXD patterns [Fig. 5(b, c)]. The fiberlike pattern of PET drawn at $T_g + 15$°C was indicative of strain-induced crystallization.[28] Drawing PET at $T_g + 30$°C resulted in a nearly isotropic WAXD pattern with weak rings corresponding to those of thermally crystallized PET. At this temperature, molecular relaxation was fast enough that PET crystallized from an essentially isotropic melt. Drawing at and above T_g is re-

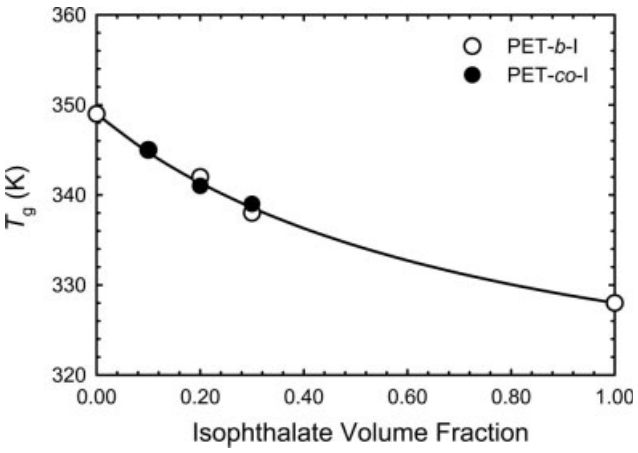

Figure 4 Effect of composition on the glass transition temperature. The data points are fit to eq. (6) (solid line) with $K = 2.0$.

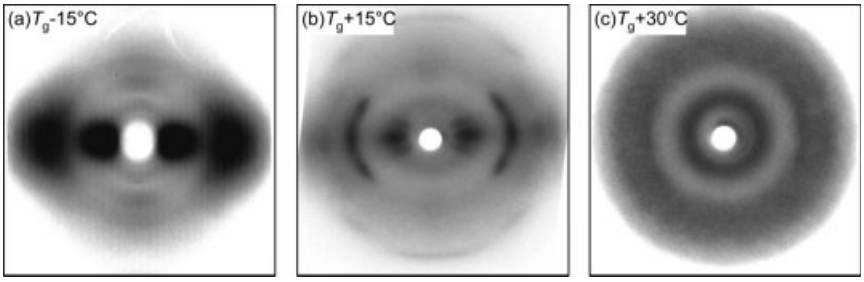

Figure 5 X-ray diffraction patterns of drawn PET films: (a) T_g − 15°C; (b) T_g + 15°C; (c) T_g + 30°C.

ferred to as hot-drawing; films drawn under these conditions contain strain-induced or thermally induced crystallinity.

The blocky copolymers oriented much more readily than the random copolymers. At T_g − 15°C and T_g, the blocky copolymers could be oriented at the same draw rate as PET, whereas a lower draw rate was required for the random copolymers.

Orientation at or below T_g + 15°C resulted in densification. For all polymers, the change in density increased with the draw-temperature (Figure 6). In contrast, drawing at T_g + 30°C produced films with much less densification. Considering the effect of composition, densification was largest for PET and decreased as the isophthalate concentration increased. In general, densification was somewhat greater for a blocky copolymer than for a random copolymer of the same composition, especially at the lower draw temperatures, which was consistent with the tendency of the blocky copolymers to orient more easily than the random copolymers.

Both orientation and crystallization of the amorphous glass result in transformation of the ethylene glycol conformation from *gauche* to *trans*.[29] Specific bands occur in the infrared spectrum of PET that are assigned to *trans* and *gauche* conformers. The ethylene glycol regions of the copolymer spectra closely resembled those of PET, and band assignments were made accordingly. The *trans* band at 1477 cm^{-1} and the *gauche* band at 1457 cm^{-1} were used for quantitative determination of conformer populations. Comparing spectra of PET, PET-*co*-30I, and PET-*b*-30I drawn at different temperatures, the intensity of the *trans* band gradually increased as the draw temperature increased from T_g − 15 to T_g + 15°C and then decreased at T_g + 30°C (Figure 7). This trend paralleled the change in density for the drawn films.

Spectra were normalized to the carbonyl band at 1730 cm^{-1},[30] and the 1500–1400 cm^{-1} region was deconvoluted into three Gaussian peaks to obtain the peak intensities. The fractions of *gauche* and *trans* conformers were determined from the normalized peak heights as described previously.[12] The results for *trans* fraction f_t are tabulated in Table IV. Drawing at

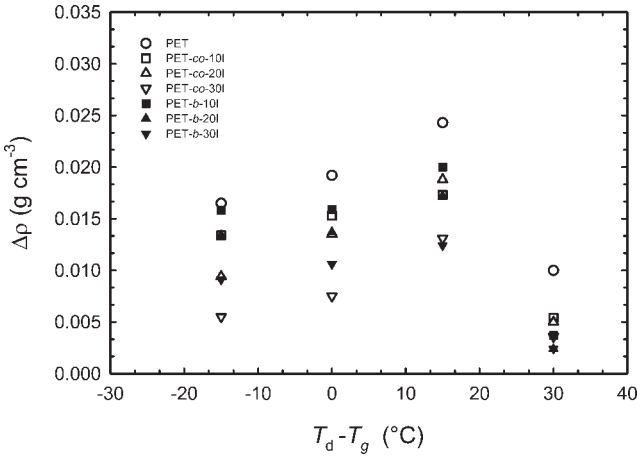

Figure 6 Density increase of drawn polyester films as a function of the draw temperature T_d relative to T_g.

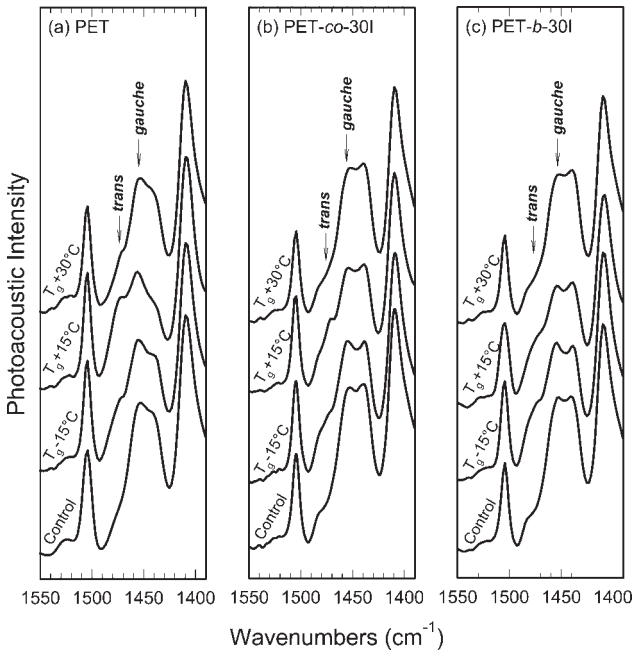

Figure 7 The 1500–1400 cm^{-1} region of the infrared spectrum of the isotropic quenched film (control) and films drawn at different temperatures relative to T_g: (a) PET; (b) PET-*co*-30I; (c) PET-*b*-30I

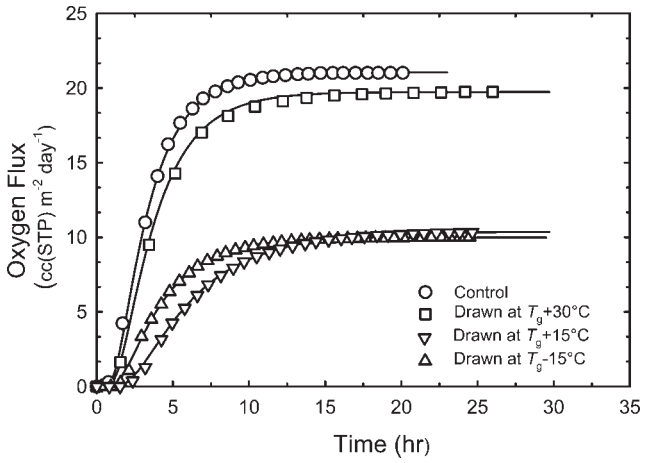

Figure 8 Experimental $J(t)$ data with the fit to eq. (8) (solid lines) for the isotropic quenched PET film (control) and PET films drawn at different temperatures relative to T_g.

$T_g - 15$°C increased f_t due to chain orientation. Drawing at T_g and $T_g + 15$°C increased f_t more due to the combined effects of amorphous phase orientation and strain-induced crystallization. The slight increase in f_t after drawing at $T_g + 30$°C was due to thermal crystallization of the relaxed melt. Blocky copolymers generally exhibited slightly higher f_t after orientation than random copolymers of the same composition.

Oxygen transport properties

Typical experimental $J(t)$ curves in Figure 8 describe the oxygen flux through films of PET quenched and drawn at various temperatures. To facilitate comparisons among specimens that varied somewhat in thickness, the flux curves were normalized to a film thickness of 200 μm using P and D calculated from the original film thickness. The initial increase in oxygen flux reflected non-steady-state diffusion. This part of the curve was controlled mainly by the diffusivity D. As the permeant concentration in the specimen reached a constant distribution, the flux reached the steady-state value J_0. This value, normalized to both the film thickness l and the permeant gas pressure p, defined the permeability $P = J_0 l p^{-1}$. Cold-drawing at $T_g - 15$°C affected both the non-steady-state and the steady-state parts of the oxygen–flux curve. The non-steady-state region broadened (slower diffusion) and the flux decreased (lower permeability). Increasing the draw temperature to $T_g + 15$°C did not affect the flux; however, the non-steady-state region broadened further. Drawing at $T_g + 30$°C had almost no effect on the oxygen flux. Both steady-state and non-steady-state regions of the flux curve were almost the same as for the quenched PET film.

To obtain the diffusivity D and to accurately determine the permeability P, the data were fit to the solution of Fick's second law with appropriate boundary conditions,[9]

$$J(t) = \frac{Pp}{l}\left[1 + 2\sum_{n=1}^{\infty}(-1)^n \exp\left(-\frac{D\pi^2 n^2 t}{l^2}\right)\right]. \quad (8)$$

The fitting curves are included with the experimental points in Figure 8. The fit was equally good for all the experiments in the study. Solubility S was calculated from the relationship $S = PD^{-1}$.

Within experimental error, P and D of blocky and random copolymers decreased logarithmically with isophthalate content (Table IV). The trend conformed to previous reports on other copolyesters.[1] Blocky copolymers had slightly lower P than random copolymers of the same composition due to slightly lower D. Drawing between $T_g - 15$°C and $T_g + 15$°C significantly reduced the oxygen permeability of PET and the copolymers (Figure 9). Lower P was due to decreases in both D and S. Drawing largely removed the effect of isophthalate on P. The lower initial P of copolymers with higher isophthalate content was offset by a smaller change in P after drawing. Draw temperature between $T_g - 15$°C and $T_g + 15$°C had almost no effect on P. A decrease in D with increasing draw temperature was offset by an increase in S. In contrast to the large decrease in P that was obtained by drawing between $T_g - 15$ and $T_g + 15$°C, drawing at $T_g + 30$°C reduced P only slightly. Somewhat lower D compared to the isotropic quenched film was offset by somewhat higher S.

DISCUSSION

A linear relationship between oxygen solubility at 25°C and 1 atm and specific volume ν has been observed for glassy copolymers of PET[1] and for cold-drawn PEN, PET, and a PET copolymer.[12] The general correlation between S and ν is expressed as

$$S = \beta(\nu - \nu_0), \quad (9)$$

where ν_0 is the specific volume at zero solubility. According to free volume concepts that view sorption as the process of filling holes of static free volume, the quantity $(\nu - \nu_0)$ identifies the excess-hole free volume available to oxygen.[1,12] The slope reflects the density of sorbed oxygen.[1]

The solubility S is plotted against specific volume ν in Figure 10 with the linear S–ν correlation previously defined for PET and numerous copolymers based on PET.[1,12] Because the trends were the same for all the copolymers, the symbols in the figure identify the draw temperature. Values for quenched films lay on the previously defined linear correlation. The decrease

TABLE IV
Physical Properties of Drawn Films

Polymer	T_d (°C)	Draw rate (mm min^{-1})	λ	ρ (g cm^{-3})	P	D	S	f_t
PET	—	—	1.0	1.3370	0.424	5.0	0.098	0.08
	T_g−15	5	4.0	1.3535	0.203	4.1	0.058	0.26
	T_g	5	4.0	1.3562	0.205	3.1	0.077	0.32
	T_g+15	20	4.1	1.3613	0.211	2.8	0.086	0.35
	T_g+30	20	6.0	1.3470	0.401	4.6	0.100	0.16
PET-*co*-10I	—	—	1.0	1.3396	0.371	4.5	0.095	0.09
	T_g−15	5	4.0	1.3530	0.170	3.3	0.059	0.28
	T_g	5	4.3	1.3549	0.165	2.6	0.074	0.25
	T_g+15	20	4.0	1.3569	0.196	2.6	0.086	0.27
	T_g+30	20	6.0	1.3450	0.325	3.7	0.103	0.15
PET-*co*-20I	—	—	1.0	1.3406	0.294	4.0	0.085	0.10
	T_g−15	2	4.0	1.3500	0.175	3.3	0.061	0.23
	T_g	5	4.0	1.3541	0.172	2.9	0.068	0.26
	T_g+15	20	4.3	1.3594	0.150	2.1	0.081	0.27
	T_g+30	20	8.0	1.3456	0.270	3.1	0.101	0.13
PET-*co*-30I	—	—	1.0	1.3410	0.249	3.5	0.082	0.11
	T_g−15	1	4.0	1.3465	0.165	2.7	0.071	0.15
	T_g	3	4.0	1.3485	0.170	2.6	0.077	0.21
	T_g+15	20	4.4	1.3541	0.138	1.9	0.083	0.26
	T_g+30	20	7.3	1.3446	0.234	2.8	0.097	0.12
PET-*b*-10I	—	—	1.0	1.3388	0.328	4.1	0.092	0.08
	T_g−15	5	4.0	1.3546	0.165	3.2	0.059	0.29
	T_g	5	4.0	1.3547	0.173	2.7	0.074	0.27
	T_g+15	20	4.1	1.3588	0.172	2.3	0.085	0.30
	T_g+30	20	6.0	1.3425	0.290	3.2	0.105	0.14
PET-*b*-20I	—	—	1.0	1.3406	0.278	3.8	0.084	0.09
	T_g−15	5	4.0	1.3540	0.175	3.2	0.064	0.28
	T_g	5	4.1	1.3543	0.154	2.5	0.072	0.29
	T_g+15	20	4.2	1.3578	0.140	2.0	0.082	0.30
	T_g+30	20	7.3	1.3430	0.250	2.9	0.101	0.13
PET-*b*-30I	—	—	1.0	1.3429	0.239	3.3	0.083	0.11
	T_g−15	5	4.0	1.3520	0.145	2.7	0.063	0.26
	T_g	5	4.1	1.3535	0.140	2.3	0.069	0.25
	T_g+15	20	4.5	1.3553	0.137	2.0	0.080	0.28
	T_g+30	20	5.3	1.3453	0.215	2.7	0.092	0.14
PEI	—	—	1.0	1.3464	0.090	1.7	0.061	0.25

Note. P, cc(STP) cm m^{-2} day^{-1} atm^{-1}; *D,* 10^{-13} m^2 s^{-1}; *S,* cc(STP) cm^{-3} atm^{-1}.

in S of cold-drawn copolymers (T_g − 15°C) followed the densification line of PET, which conformed to the previous understanding that orientation by cold-drawing removed excess free volume as measured by S. The single correlation led to the common zero-solubility specific volume ν_0 for all the copolymers. Increasing the draw temperature from T_g − 15°C to T_g tended to increase S with almost no decrease in ν. Increasing the draw temperature further to T_g + 15°C led to a further increase in S with a slight decrease in ν. Finally, drawing at T_g + 30°C increased S more and also increased ν. As a result, S of hot-drawn films (T_g to T_g + 30°C) lay systematically above the S–ν correlation. It appeared that strain-induced crystallization had a complex effect on the final structure that determined S.

Transport behavior of crystalline PET is often considered in terms of a two-phase structure consisting of an impermeable crystalline phase dispersed in a permeable amorphous matrix. Thus, both sorption and diffusion are seen as taking place in the amorphous phase. It follows that solubility of the amorphous phase S_a is given by

$$S_a = \frac{S}{1 - \phi_c}, \tag{10}$$

where ϕ_c is the volume fraction crystallinity. Furthermore, eq. (9) can be written for the amorphous phase of crystallized PET[31] and other polyesters[29] as

$$S_a = \beta(\nu_a - \nu_0). \tag{11}$$

Whereas orientation of the glassy state decreases the excess-hole free volume ($\nu_f = \nu_a - \nu_0$), crystallization often has the effect of increasing the excess-hole free volume of the amorphous phase.

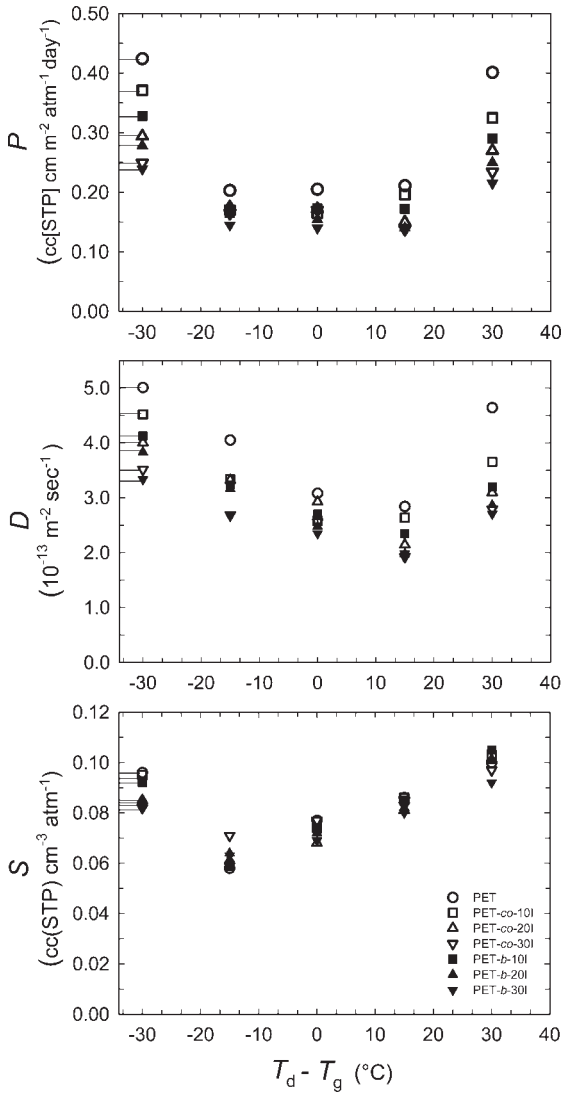

Figure 9 Effect of draw temperature on oxygen-transport properties of drawn polyesters: (a) permeability; (b) diffusivity; and (c) solubility. Values for the isotropic quenched films (controls) are indicated on the ordinate.

Following the approach used with PET,[10] the two-phase model is expressed in terms of density as

$$\rho = \rho_c \phi_c + \rho_a(1 - \phi_c)\,, \tag{12}$$

with a constant crystalline phase density ρ_c taken as 1.476 g cm^{-3}, which is considered intrinsic for the defective crystalline phase in PET,[32] and a variable amorphous phase density $\rho_a(\rho)$.

Equations (10), (11), and (12) can be solved simultaneously for ρ_a, ϕ_c, and S_a with known constants β (3.6 cc(STP) g cm^{-6} atm^{-1}), ν_0 (0.722 cm^3 g^{-1}), and ρ_c (1.476 g cm^{-3}) and experimentally determined S and ρ. The results for ρ_a, ϕ_c, and S_a are summarized in Table V. The results are not particularly sensitive to the choice of ρ_c. For example, changing ρ_c from 1.476 to 1.496 g cm^{-3} changes ϕ_c by about 0.02 and ρ_a by less than 0.001 g cm^{-3}. However, ϕ_c is particularly sensitive to ρ_a. For example, decreasing ρ_a from 1.335 to 1.315 g cm^{-3} increases ϕ_c from 0.21 to 0.31 for ρ of 1.365 g cm^{-3}.

The calculated value of ϕ_c increased from 0 for films drawn at T_g − 15°C to a maximum for films drawn at T_g + 15°C and then decreased somewhat in films drawn at T_g + 30°C. The maximum value obtained for ϕ_c tended to decrease as the isophthalate content increased; however, there were no significant differences between the blocky and random copolymers. Increasing the draw temperature progressively densified the amorphous phase over the entire temperature range studied, as shown by the monotonic decrease in ρ_a (Figure 11, and the corresponding increase in S_a (Table V). However, it is noteworthy that between T_g − 15°C and T_g + 15°C, P remained relatively unaffected by draw temperature because increasing S_a was offset by decreasing D due to strain-induced crystallization.

A previous study found that changes in amorphous density correlated with changes in the ethylene glycol conformation.[12] To test the relationship for oriented polymers with strain-induced crystallization, the amorphous *trans* fraction was estimated by assuming that glycol units in the crystalline phase were entirely in the *trans* conformation. Subtracting the weight fraction crystallinity w_c from the total *trans* fraction f_t gave the amorphous *trans* fraction $f_{t,a}$ as

$$f_{t,a} = f_t - w_c\,. \tag{13}$$

The relationship between ρ_a and $f_{t,a}$ in Figure 12 followed the correlation previously established for cold-drawn PET.[12] Extrapolation led to densities of 1.323 and 1.420 g cm^{-1} for *gauche* and *trans* conformers,

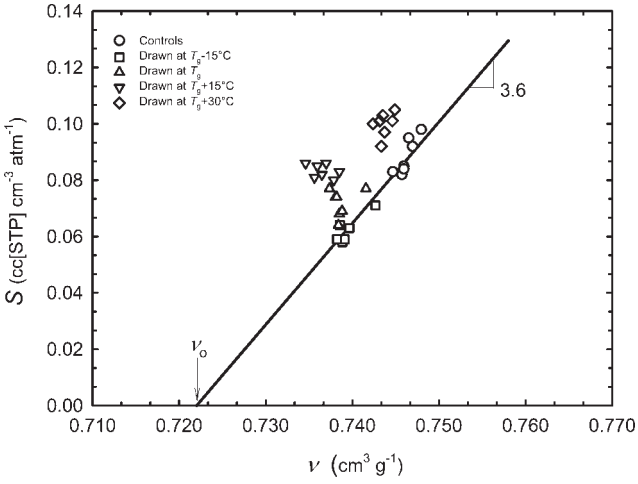

Figure 10 Relationship between oxygen solubility and specific volume ($\nu = \rho^{-1}$) for isotropic quenched films (controls) and drawn films.

TABLE V
Amorphous Phase Properties of Drawn Films

Polymer	T_d (°C)	ρ (g cm^{-3})	ρ_a (g cm^{-3})	ϕ_c	S_a	$f_{t,a}$	v_f (cm^3 g^{-1})
PET	—	1.3370	1.337	0.00	0.098	0.08	0.026
	T_g−15	1.3535	1.354	0.00	0.058	0.26	0.017
	T_g	1.3562	1.340	0.12	0.088	0.20	0.024
	T_g+15	1.3613	1.329	0.22	0.110	0.13	0.030
	T_g+30	1.3470	1.322	0.16	0.119	0.00	0.034
PET-*co*-10I	—	1.3396	1.340	0.00	0.095	0.09	0.024
	T_g−15	1.3530	1.353	0.00	0.059	0.28	0.017
	T_g	1.3549	1.343	0.09	0.081	0.16	0.023
	T_g+15	1.3569	1.331	0.18	0.105	0.09	0.029
	T_g+30	1.3450	1.324	0.14	0.120	0.01	0.033
PET-*co*-20I	—	1.3406	1.341	0.00	0.085	0.10	0.024
	T_g−15	1.3500	1.350	0.00	0.061	0.23	0.019
	T_g	1.3541	1.345	0.07	0.073	0.19	0.022
	T_g+15	1.3594	1.334	0.18	0.099	0.09	0.028
	T_g+30	1.3456	1.326	0.13	0.116	0.00	0.032
PET-*co*-30I	—	1.3410	1.341	0.00	0.082	0.11	0.024
	T_g−15	1.3465	1.347	0.00	0.071	0.15	0.021
	T_g	1.3485	1.343	0.04	0.080	0.17	0.022
	T_g+15	1.3541	1.336	0.13	0.095	0.13	0.027
	T_g+30	1.3446	1.330	0.10	0.108	0.02	0.030
PET-*b*-10I	—	1.3388	1.339	0.00	0.092	0.08	0.025
	T_g−15	1.3546	1.355	0.00	0.059	0.29	0.016
	T_g	1.3547	1.343	0.09	0.081	0.18	0.023
	T_g+15	1.3588	1.331	0.19	0.105	0.11	0.029
	T_g+30	1.3425	1.324	0.12	0.119	0.02	0.033
PET-*b*-20I	—	1.3406	1.341	0.00	0.084	0.09	0.024
	T_g−15	1.3540	1.354	0.00	0.064	0.28	0.017
	T_g	1.3543	1.345	0.07	0.077	0.22	0.021
	T_g+15	1.3578	1.335	0.16	0.098	0.14	0.027
	T_g+30	1.3430	1.328	0.10	0.112	0.03	0.031
PET-*b*-30I	—	1.3429	1.343	0.00	0.083	0.11	0.023
	T_g−15	1.3520	1.352	0.00	0.063	0.27	0.018
	T_g	1.3535	1.347	0.05	0.073	0.20	0.020
	T_g+15	1.3553	1.339	0.12	0.091	0.16	0.025
	T_g+30	1.3453	1.334	0.08	0.100	0.07	0.028
PEI	—	1.3464	1.346	0.00	0.061	0.25	0.021

Note. S_a, cc(STP) cm^{-3} atm^{-1}.

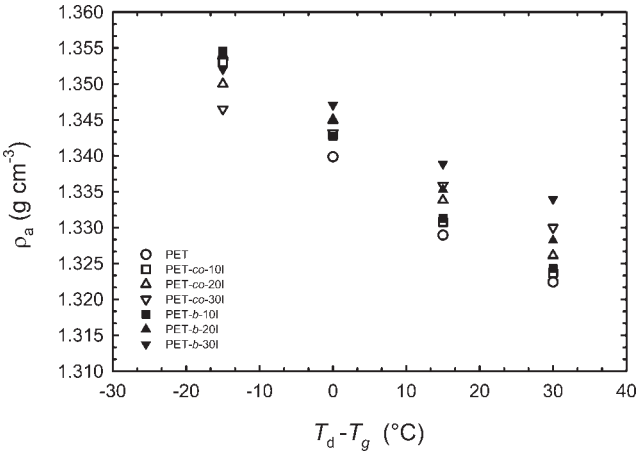

Figure 11 Amorphous phase density plotted versus draw temperature relative to T_g.

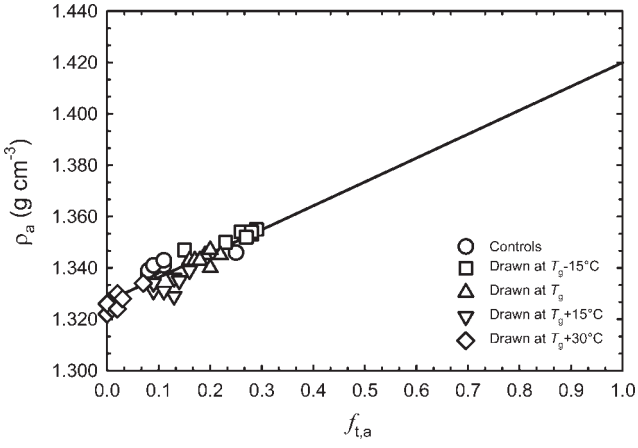

Figure 12 Relationship between amorphous phase density and amorphous phase *trans* fraction for isotropic quenched films (controls) and drawn films.

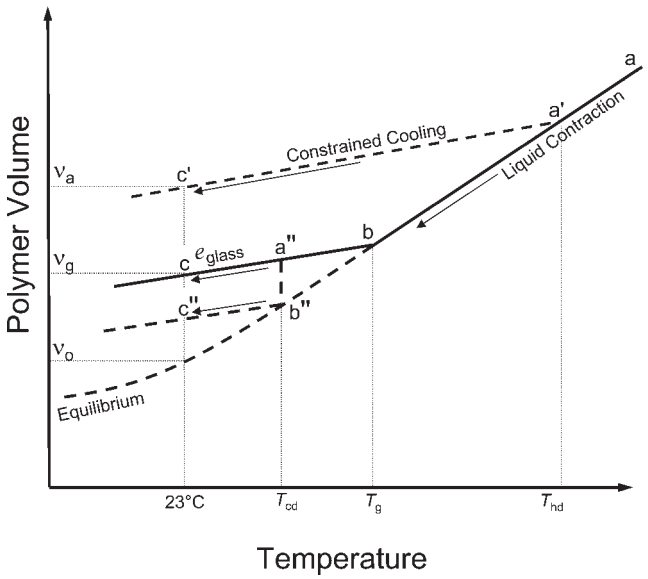

Figure 13 Relationship between temperature and amorphous specific volume for PET.

respectively. The correlation revealed that the *trans* fraction $f_{t,a}$ determined the chain packing in both densified cold-drawn amorphous films and dedensified amorphous phase of hot-drawn films with strain-induced crystallization. Coincidentally, the amorphous density of films drawn at T_g + 30°C, 1.32–1.33 g cm^{-3}, conformed to the all-*gauche* conformer density, suggesting that all the *trans* conformers were incorporated into crystals.

An increase in specific volume of the amorphous phase with crystallization is attributed to constraint on relaxation of amorphous chain segments imposed by their attachment to chain segments in crystals.[29] The effect of constraint on amorphous chains can be discussed in terms of the temperature–volume relationship in Figure 13. During cooling, unconstrained amorphous chains contract along the equilibrium liquid line (ab in Fig. 13) to the normal glass transition temperature T_g, and then along the unconstrained nonequilibrium glassy line (bc in Fig. 13) to ambient temperature. Hot-drawing at or above T_g induces crystallization. The remaining amorphous chain segments are attached to chain segments in crystals. As the film is cooled from the hot-draw temperature T_{hd}, amorphous chain segments lack mobility to relax along the liquid line; instead, they are immobilized much as they would be in the glassy state. During cooling from T_{hd}, contraction along a line parallel to the normal glassy line (a′c′ in Fig. 13) increases the hole free volume, bringing the nonequilibrium glass further from the equilibrium line. The additional hole free volume resulting from constraint $\Delta\nu_f$ is the difference between the dedensified amorphous specific volume ν_a and the specific volume of the unconstrained glass ν_g. It follows from the concept of the amorphous phase as presented in Figure 13 that the glass transition temperature should increase with dedensification. Indeed, this has been observed in blown bottle walls.[8]

The effective glass transition temperature T'_g, which should be equal to the nominal draw temperature T_d, can be derived from the temperature–volume relationship and ν_a according to T'_g.

$$T'_g = T_g + \frac{\nu_a - \nu_g}{\Delta e}, \tag{14}$$

where Δe is the difference between the specific thermal expansivities of equilibrium liquid and glass, taken as 3.0×10^{-4} cm^3 g^{-1} K^{-1}, T_g is the normal glass transition temperature of PET taken as 76°C, and ν_g is the specific volume of glassy PET taken as 0.748 cm^3 g^{-1}. Calculated values of T'_g from eq. (14) are compared with the draw temperature in Figure 14. Excellent correlation supports the concept of amorphous constraint as presented in Figure 13 and confirms the key role of draw temperature in determining the amorphous phase properties of the drawn polymer.

Orientation by cold-drawing decreases the hole free volume, bringing the nonequilibrium glass closer to the equilibrium line.[12,33] It is noteworthy that results for cold-drawn copolymers fall close to the identity line in Figure 14. According to the concept of the amorphous phase as presented in Figure 13, cold-drawing at T_{cd} brought the glass to the equilibrium cooling curve at the draw temperature (a″b″ in Fig. 13), followed by contraction along a line parallel to the normal glassy line (b″c″ in Fig. 13). It follows that T_g

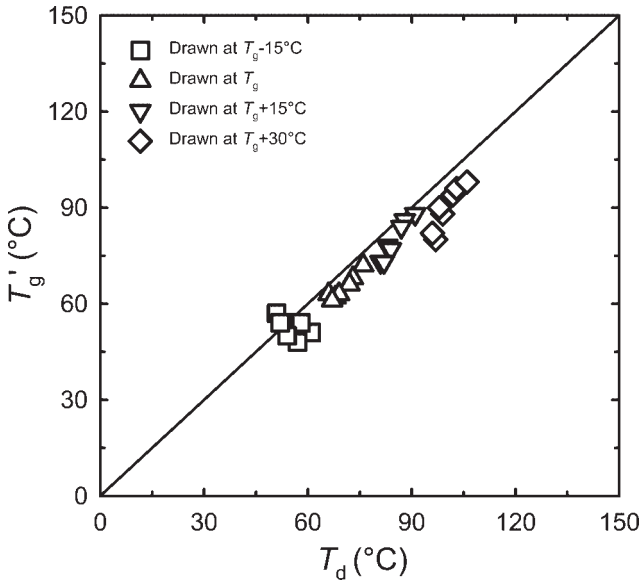

Figure 14 Correlation between draw temperature and effective glass transition temperature from eq. (14).

should decrease with densification of the glass. Indeed, the T_g inflection of copolymers drawn at $T_g - 15°C$ was somewhat lower than the normal T_g of the glass.[8] Although this interpretation suggests that drawing at any temperature below T_g would bring the polymer to the equilibrium cooling curve, such a possibility seems highly unlikely. To the authors' knowledge, a density of 1.385 g cm^{-1}, i.e., the density of the glass at 23°C with no excess-hole free volume, has not been achieved by drawing PET at ambient temperature.

CONCLUSIONS

This study demonstrates that transesterification of PET and PEI blends is slow enough that the normal processes of melt blending and compression molding produce a substantially blocky copolymer. Observation of a single glass transition for random and blocky copolymers indicates miscibility of PET and PEI blocks in the glassy state. However, the difference in isophthalate distribution leads to a major difference in crystallization from the glass. Random distribution of isophthalate units significantly retards crystallization. In contrast, blocky copolymers with up to 30% isophthalate crystallize rapidly to achieve a total crystallinity close to that of PET.

Orientation of all the copolymers resulted in property changes consistent with strain-induced crystallization. However, blocky copolymers oriented more easily than random copolymers of the same composition, and after orientation they exhibited slightly lower oxygen permeability, higher density, and higher fraction *trans* conformers.

Oxygen permeability of random and blocky copolymers in the unoriented, glassy state decreases logarithmically with isophthalate content. Orientation at or near the glass transition temperature significantly reduces oxygen permeability of all the polymers, although the effect lessens as the isophthalate content increases. As a result, isophthalate content and distribution have only subtle effects on oxygen permeability after orientation to a target draw ratio of 4.

Although oxygen permeability does not depend on draw temperature in the vicinity of the glass transition ($T_g \pm 15°C$), diffusivity and solubility, which together determine the permeability, do change with draw temperature. Decreasing oxygen diffusivity is offset by increasing oxygen solubility. Analysis of oxygen solubility by free volume concepts reveals the amount of crystallinity and fundamental characteristics of the amorphous phase, such as amorphous phase density and amorphous phase oxygen solubility. Dedensification of the amorphous phase is due to constraint on amorphous chains attached to chain segments in crystals. The amount of dedensification correlates with increasing population of *gauche* ethylene glycol conformers in the amorphous phase. The strong dependence of dedensification on draw temperature is explained in terms of the temperature–volume relationship of the amorphous phase. As was demonstrated elsewhere with PET bottle walls,[8] this methodology provides a valuable nondestructive tool for probing the structure of drawn polyester films.

References

1. Polyakova, A.; Liu, R. Y. F.; Schiraldi, D. A.; Hiltner, A.; Baer E. J Polym Sci Part B: Polym Phys 2001, 39, 1889.
2. Light, R. R.; Seymour, R. W. Polym Eng Sci 1982, 22, 857.
3. Lee, S. W.; Ree, M.; Park, C. E.; Jung Y. K.; Park, C. S.; Jin, Y. S.; Bae, D. C. Polymer 1999, 40, 7137.
4. Swaroop, N.; Gordon, G. A. Polym Eng Sci 1980, 20, 78.
5. Kint, D. P. R.; Martínez de Ilarduya, A.; Sansalvadó, A.; Ferrer, J; Muñoz-Guerra, S. J Appl Polym Sci 2003, 90, 3076,
6. Liu, R. Y. F.; Hu, Y. S.; Hibbs, M. R.; Collard, D. M.; Schiraldi, D. A.; Hiltner, A.; Baer, E. J Polym Sci Part B: Polym Phys 2003, 41, 289.
7. Hiltner, A.; Liu, R. Y. F.; Hu, Y. S.; Baer, E. J.; Polym Sci Part B: Polym Phys 2005, 43, 1047.
8. Liu, R. Y. F.; Hu, Y. S.; Schiraldi, D. A.; Hiltner, A.; Baer, E. J Appl Polym Sci 2004, 94, 671.
9. Sekelik, D. J; Stepanov, S.V.; Nazarenko, S.; Schiraldi, D.; Hiltner, A.; Baer, E. J Polym Sci Part B: Polym Phys 1999, 37, 847.
10. Qureshi, N.; Stepanov, E. V.; Schiraldi, D.; Hiltner, A.; Baer, E. J Polym Sci Part B: Polym Phys 2000, 38, 1679.
11. Cheng, S. Z. D.; Cao, M.–Y.; Wundelich, B. Macromolecules 1986, 19, 1868.
12. Liu, R. Y. F.; Schiraldi, D. A.; Hiltner, A.; Baer, E. J Polym Sci Part B: Polym Phys 2002, 40, 862.
13. Kluin, J.-E.; Yu, Z.; Vleeshouwers, S.; McGervey, J. D.; Jamieson, A. M.; Simha, R.; Sommer, K. Macromolecules 1993, 26, 1853.
14. Martinez de Ilarduya, A.; Kint, D. P. R.; Munoz-Guerra, S. Macromolecules 2000, 33, 4596.
15. Kint, D. P. R.; Martinez de Ilarduya, A.; Munoz-Guerra, S. Macromolecules 2002, 35, 314.
16. Herbert, I. R.; In NMR Spectroscopy of Polymers; Ibbett, R. N. Ed.; Blackie Academic and Professional: London, 1993; Chapter 2, p 50.
17. Chen, H. Y.; Stepanov, E. V.; Chum, S. P.; Hiltner, A.; Baer, E. Macromolecules 2000, 33, 8870.
18. Karayiannis N. C.; Mavrantzas, V. G.; Theodorou, D. N. Macromolecules 2004, 37, 2978.
19. Yip, H. K.; Williams, H. L. J Appl Polym Sci 1976, 20, 1217.
20. Tonelli, A. E. J Polym Sci Part B: Polym Phys 2002, 40, 1254.
21. Polyakova, A.; Connor, D. M.; Collard, D. M.; Schiraldi, D. A.; Hiltner, A.; Baer, E. J Polym Sci Part B: Polym Phys 1900, 2001, 39.
22. Gordon, M.; Taylor, J. S. J Appl Chem 1952, 2, 493.
23. Couchman, P. R.; Karasz, F. E. Macromolecules 1978, 11, 117.
24. Van Krevelen, D. W.; Properties of Polymers, 3rd ed.; Elsevier: Amsterdam, 1997.
25. Karayannidis, G. P.; Sideridou, I. D.; Zamboulis, D. N.; Bikiaris, D. N.; Sakalis, A. J Polym Sci B Polym Phys 2000, 78, 200.
26. Armeniades, C. D.; Baer, E. J Polym Sci A-2 1971, 9, 1345.
27. Tonelli, A. E. Polymer 2002, 43, 637.
28. Fischer, E. W.; Fakirov, S. J Mater Sci 1976, 11, 1041.
29. Hu, Y. S.; Liu, R. Y. F.; Zhang, L. Q.; Rogunova, M.; Schiraldi, D. A.; Nazarenko, S.; Hiltner, A.; Baer, E. Macromolecules 2002, 35, 7326.
30. Cole, K. C.; Ben Daly, H.; Sanschagrin, B.; Nguyen, K. T.; Ajji, A. Polymer 1999, 40, 3505.
31. Polyakova, A.; Stepanov, E. V.; Sekelik, D.; Schiraldi, D. A.; Hiltner, A.; Baer, E. J Polym Sci Part B: Polym Phys 1911, 2001, 39.
32. Bornschlegl, E.; Bonart, R. Colloid Polym Sci 1980, 258, 319.
33. Liu, R. Y. F.; Hiltner, A.; Baer, E. J. Polym Sci Part B: Polym Phys 2004, 42, 493.